TCAD Modeling of Carbon Electrode for Highly Accurate Reset Current Prediction of Phase Change Memory Considering Both Thermal and Electronic Transport

Takayuki Tsukagoshi[1], Hiroki Tokuhira[1], Tsukasa Nakai[1], Yuya Matsuzawa[2], Ryouji Masuda[2], Hironobu Furuhashi[2], Shosuke Fujii[2], Hiroyuki Ode[2], and Naoki Kusunoki[1]
[1]Institute of Memory Technology R&D, Kioxia Corporation, Yokohama, Japan
[2]Institute of Memory Technology R&D, Kioxia Corporation, Yokkaichi, Japan
Email: takayuki.tsukagoshi@kioxia.com

***Abstract*—A TCAD model considering both the electrical and thermal conductivity of a carbon electrode was developed and experimentally calibrated. The electrical conductivity was considered using the Poole conduction model, while the thermal conduction was considered as the sum of the constant phonon and electronic components expressed by the Wiedemann-Franz law. Using the developed TCAD model, we could successfully predict the reset current (*Ireset*) of phase-change material (PM)/selector stacked devices with high accuracy. The heat was generated not only in the selector but also in the top electrode (TE) of carbon, and it was confirmed that accurate modeling of both electrical and thermal conductivity of TE is indispensable for reproducing *Ireset* of a real device. Finally, side etching of the TE was demonstrated to generate increased Joule heating in the TE to decrease *Ireset*.**

***Index Terms*—Amorphous carbon, Joule heating, PCM, Poole conduction, Selector, TCAD**

I. Introduction

Phase-change memory (PCM) [1], [2], in which a phase-change material (PM) and a selector are stacked between the top electrode (TE) and bottom electrode (BE) (Fig. 1), has been developed as a candidate for cross-point memory [3], [4]. One of the challenges in device development is the reduction in the reset current (*Ireset*) required to change the PM from a crystalline state to an amorphous state. To reduce *Ireset*, the middle electrode (ME) must not block heat inflow from the selector, while the TE must be thermally insulative so that heat from the selector can be confined in the PM [4]. In addition, the memory stack must be electrically conductive. Amorphous carbon (a-C) is an electrode material that satisfies the above conditions.

It is well known that the electrical conductivity of a-C decreases with an increase in the content of sp^3C-C bonds or the N-doping concentration [5], while the thermal conductivity decreases as the film density decreases [6]. However, it has not been reported if the *Ireset* of PM/selector stacked cells with carbon electrodes can be successfully predicted using a TCAD model.

In this study, we developed a TCAD model of a carbon electrode to predict *Ireset* of PM/selector stacked devices with high accuracy for the first time and demonstrated the possibility of side etching of TE to reduce *Ireset*. Using our TCAD model, the simulation results adequately reproduced the experimental data of the TE thickness and density dependence, an alternative method to reduce *Ireset* was demonstrated.

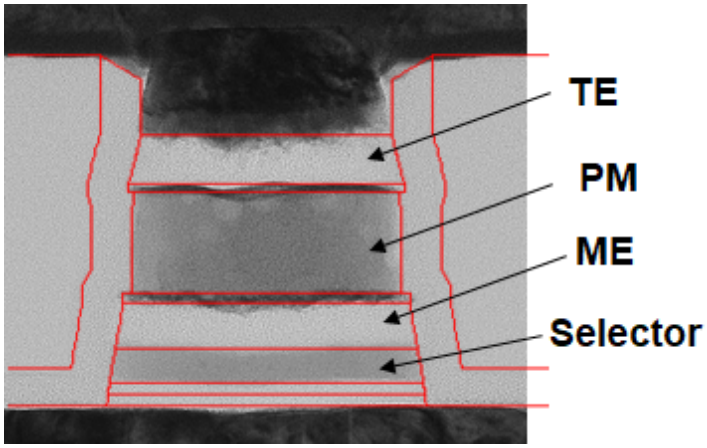

Fig. 1. Cross-sectional TEM image and simulated topography by TCAD (red line) of the PM/Selector stacked device. Simulated topography is well calibrated in the TEM image before starting the *Ireset* simulation.

II. Modeling

First, we explain the model of electrical transport in carbon films, that is Poole conduction, expressed as

$$\sigma(T,F) = \sigma_0 \exp\left(-\frac{E_a - \alpha F}{k_B T}\right) \quad (1)$$

where α is a constant and σ_0, E_a, F, k_B and T denote the electrical conductivity at high temperature, trap energy, electric field, Boltzmann constant, and temperature, respectively. This model can explain the threshold switching behavior of a-C with a high trap density [7]. To simulate the electrical characteristics of a-C with and without nitrogen doping (CNx

and Pure C), it is necessary to extract several parameters (σ_0, E_a, α) in the Poole conduction model. Fig. 2 shows the simulated and experimental I-V characteristics of the a-C films. In Fig. 2, the symbols represent the experimental data and the solid lines refer to the simulation results. It is evident that the simulation results are in good agreement with the experimental results. As a result, the Poole conduction parameters in a-C were precisely extracted in the calibration.

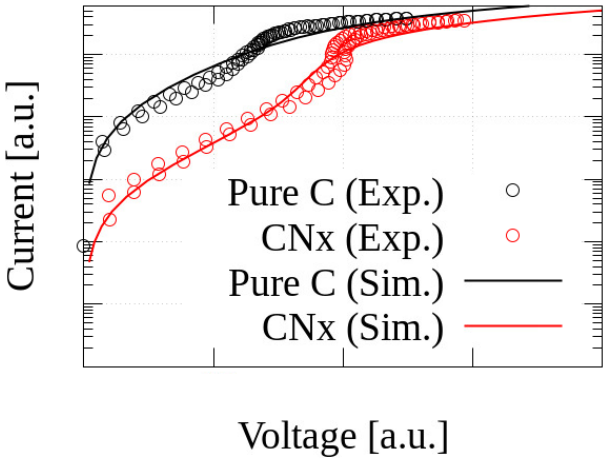

Fig. 2. Experimental and simulated current-voltage characteristics of amorphous carbon with and without nitrogen doping (CNx and Pure C). Model parameters of Poole conduction are extracted from this calibration.

Fig. 3 shows the electrical conductivity at an electric field of 0 MV/cm calculated using the above-mentioned Poole conduction model and experimental data obtained by four-terminal measurements. The TCAD model results were similar to the measured values at room temperature. In addition, the extracted trap energy (E_a) of CNx was larger than that of Pure C, indicating that the electrical conductivity of CNx is lower. This can be attributed to the formation of sp^3C-N bonds [5].

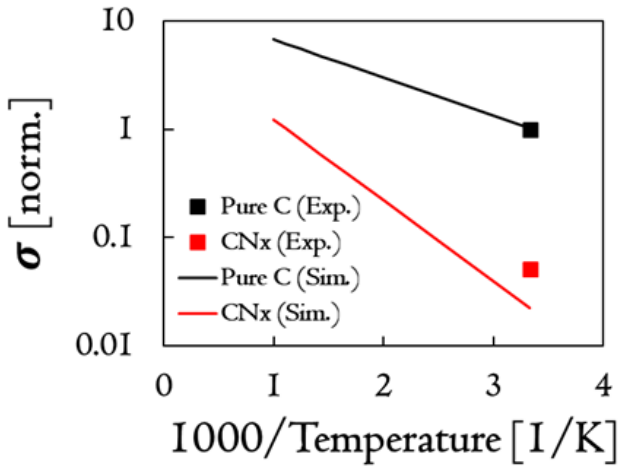

Fig. 3. Calculated electrical conductivity (σ) with model parameters extracted by I-V calibration, as shown in Fig. 2, at $E = 0$ MV/cm. Simulated σ is almost the same as the experimental data obtained by four-terminal measurements at room temperature.

Subsequently, as a heat conduction model, we consider the sum of the constant phonon and electronic components expressed by the Wiedemann-Franz law, expressed as

$$\kappa_{\text{tot}}(T, F) = \kappa_{\text{phonon}} + L \cdot \sigma(T, F) \cdot T \tag{2}$$

where L denotes the Lorentz number. Here, the phonon component (κ_{phonon}) is expressed as a proportionality formula to the film density, which is used with the values measured using the thermo-reflectance method, as shown in Fig. 4. The thermal conductivity measured by the thermo-reflectance method includes both the phonon component and electronic component; however, the latter contribution is negligible at room temperature. The linear relationship between the thermal conductivity of a-C and the film density is confirmed by 3ω measurements [6]. This implies that the thermal conductivity of a-C is related to the content of sp^3C-C bonds since the film density of a-C scales with the content of sp^3C-C bonds [8].

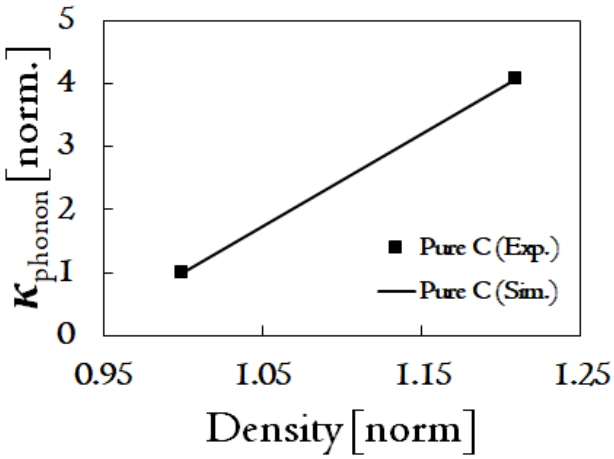

Fig. 4. Phonon-based thermal conductivity (κ_{phonon}) considering the dependence of film density measured by the thermo-reflectance method at room temperature.

Finally, we simulated *Ireset* of the PM/selector stacked device using a well-calibrated in-house simulator that implemented the phase-change model of the PM and the switching model of the selector. The thermal and electrical conductivity of the PM and selector were based on the measured data and calibrated values using the electrical data, as mentioned above. In the simulation of *Ireset*, a reset pulse was applied to the memory cell to transition it from a crystalline state to an amorphous state.

III. Results and Discussion

We show a comparison of *Ireset* between the experimental data and simulation results of the TE thickness and density dependency in Figs. 5(a) and (b). In these figures, black and red symbols represent the experimental data and simulation results, respectively. Before starting the *Ireset* simulation, we calibrated the topography of the PM/selector-stacked devices using cross-sectional TEM images, as shown in Fig. 1. Here,

the variation in shape has been included in actual devices, even when fabricated under the same conditions. Therefore, to clearly observe the influence of only the TE, shape correction was performed to obtain *Ireset* under the conditions of the same PM and ME diameters. Shape correction values calculated using TCAD were used. The simulation results obtained using our TCAD model were in good agreement with the experimental data. As shown in Fig. 5(a), as the thickness of the TE increases, *Ireset* decreases because of the increase in Joule heating in the TE. Meanwhile, as the density of the TE decreases, *Ireset* decreases owing to the suppression of heat dissipation from the TE thanks to the lower thermal conductivity, as shown in Fig. 5(b).

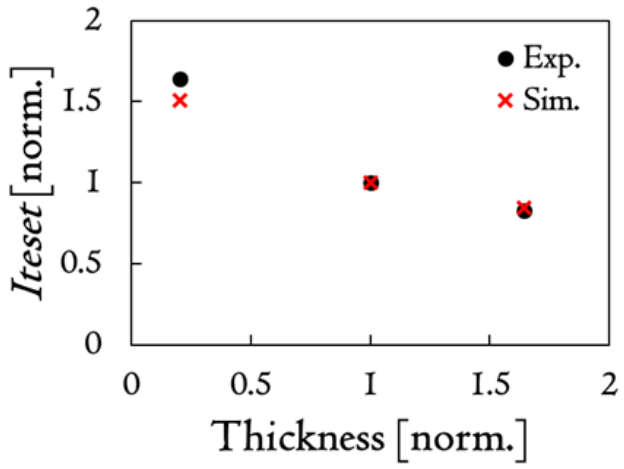

(a)

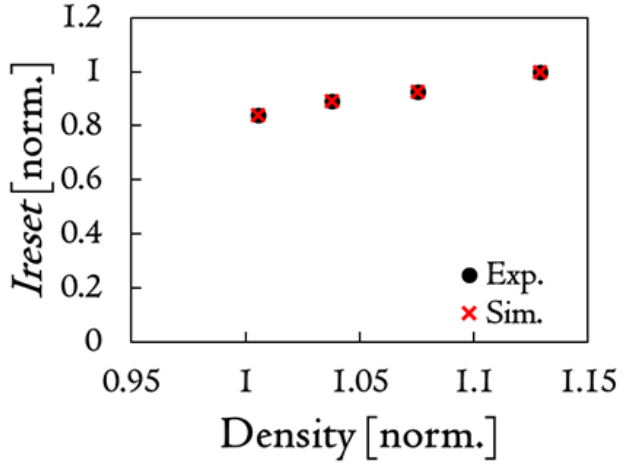

(b)

Fig. 5. Experimental and simulated *Ireset* of PM/Selector stacked devices for the dependence of (a) TE thickness and (b) density.

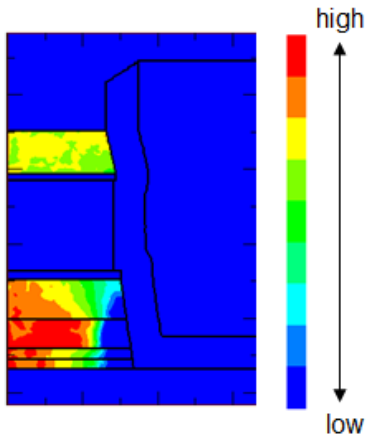

Fig. 6. Joule heating distribution in PM/Selector stacked device.

To understand the simulation results, we confirmed the Joule heating distribution in the PM/Selector-stacked device during the reset operation, as shown in Fig. 6. It can be seen that heat was generated not only in the selector but also in the TE. Therefore, we confirm that the accurate modeling of both the electrical and thermal conductivity of the TE is indispensable for reproducing the *Ireset* of a real device.

In the discussion thus far, we demonstrated two methods utilizing TE, i.e., an a-C film of higher thickness and lower density, for reducing *Ireset* and the development of a highly accurate TCAD model based on experimental data. As it is crucial to discover a method of *Ireset* reduction, we investigated the possibility of side etching of the TE, as shown in Fig. 7. Fig. 8 shows *Ireset* with different amounts of side etching, defined by the difference in width between the TE outside and PM. It was found that the larger the side etching of the TE, the lower the *Ireset*. To understand this mechanism, we show the Joule heating distribution in the PM/Selector-stacked devices under the same current conditions shown in Fig. 9. We found that the heat generation was higher at the TE because of the higher electrical resistance owing to side etching. Therefore, it was found that *Ireset* with wider side etching of the TE was reduced owing to higher Joule heating. Here, a higher resistance of the TE has the possibility of a narrow read margin; therefore, it is necessary to optimize the amount of side etching to reduce *Ireset* and obtain a sufficient read current. In other words, the modeling of electrical conductivity is inevitable for the accurate prediction of not only Joule heating but also the read current. Therefore, a TCAD model that includes both thermal and electronic transport is indispensable for read and write operations in the design of PCM.

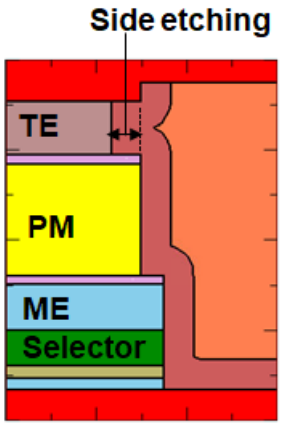

Fig. 7. Topography for investigating the impact of TE side etching for *Ireset* reduction.

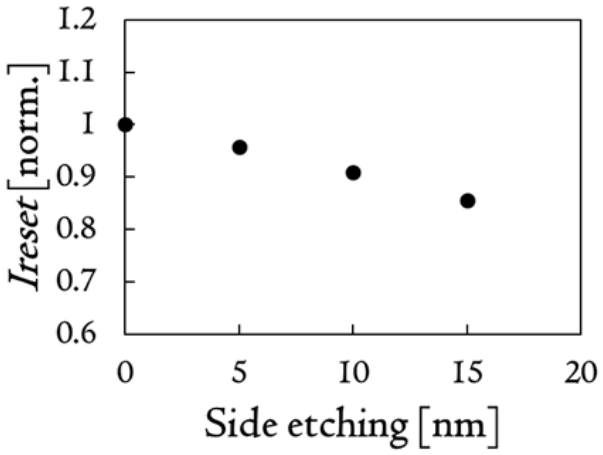

Fig. 8. Relationship between *Ireset* and side etching width of TE. The larger the side etching of TE, the lower the reset current.

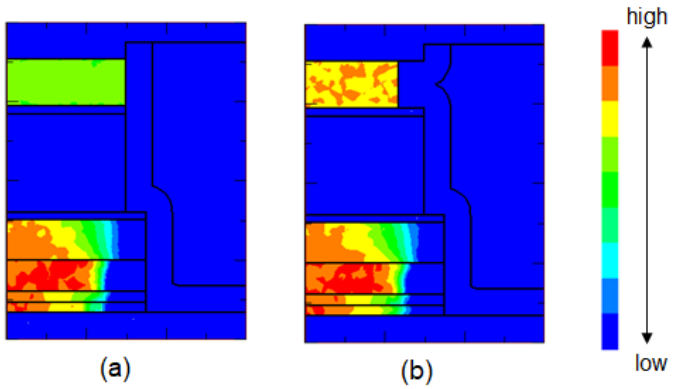

Fig. 9. Joule heating distribution in PM/Selector stacked devices without side etching of (a) TE and (b) with side etching.

IV. Conclusion

We presented a TCAD model of both the electrical and thermal conductivity of the carbon electrode. The electrical conductivity was considered as the Poole conduction model, while the thermal conduction was defined as the sum of the constant phonon and electronic components expressed by the Wiedemann-Franz law. Using our TCAD model, we demonstrated the accurate prediction of *Ireset* of PM/Selector stacked devices. Furthermore, we demonstrated a strategy for *Ireset* reduction with side etching of TE. Our model is expected to simulate the operation of phase-change memory devices.

Acknowledgment

The authors thank H. Kawai for his support during this study. The authors are grateful to the device and process integration teams for fabricating the devices. The authors are deeply grateful to H. Horii and K. Nishitani for their encouragement throughout this study.

References

[1] H.-S. Philip Wong *et al.*, "Phase Change Memory," Proceedings of the IEEE vol. 98, 2010, pp. 2201–2227.

[2] Geoffrey W. Burr *et al.*, "Phase change memory technology," Journa of Vacuum Science & Technology B vol. 28, 2010, pp. 223–262.

[3] Kim *et al.*, "High-performance, cost-effective 2z nm two-deck cross-point memory integrated by self-align scheme for 128 Gb SCM," 2018 IEEE International Electron Devices Meeting (IEDM), San Francisco, CA, USA, 2018, pp. 37.1.1–37.1.4.

[4] Y. Matsuzawa *et al.*, "One-Pulse-Programmable Multi-Level PCM/Selector Cross-Point Memory for 20 nm Half Pitch and Beyond," IEEE 53rd European Solid-State Device Research Conference (ESSDERC) Lisbon, Portugal, 2023, in press.

[5] N. Tamura *et al.*, "DC electricai conductivity study of amorphous carbon nitride fiims prepared by reactive RF rnagnetron sputtering," Japanese Journal of Applied Physics vol. 53, 2014, pp. 02BC03-1–02BC03-4.

[6] M. Shamsa *et al.*, "Thermal conductivity of diamond-like carbon films," Applied Physics Letters vol. 89, 2006, pp. 161921-1–161921-3.

[7] A. Sebastian *et al.*, "Resistance switching at the nanometre scale in amorphous carbon," New Journal of Physics vol. 13, 2011, p. 013020.

[8] A. C. Ferrari *et al.*, "Density, sp^3 fraction, and cross-sectional structure of amorphous carbon films determined by x-ray reflectivity and electron energy-loss spectroscopy," Physical Review B vol. 62, 2000, pp. 11089-11103.